Int. J. Rock Mech. Min. Sci. & Geomech. Abstr. Vol.30, No.7, pp. 1285–1290, 1993
Printed in Great Britain

0148-9062/93 $6.00 + 0.00
Pergamon Press Ltd

Mechanics of a Rock Anchor with a Penny-shaped Basal Crack

A.P.S. SELVADURAI[1]

The present paper examines the linear elastostatic problem related to a cylindrical elastic anchor which is embedded in partial bonded contact with an elastic medium. The base of the elastic anchor contains a flat circular crack, the boundary of which extends beyond the elastic anchor. The analysis focusses on the utilization of the boundary element technique for the evaluation of the axial stiffness of the anchor and the stress intensity factors at the boundary of the crack.

INTRODUCTION

In the classical formulation of the near surface anchor problem it is usually assumed that there is perfect bonding between the anchoring element and the elastic medium with the resulting continuity of displacements and tractions at the interface. In many practical situations involving relatively long flexible anchoring devices, this assumption is realized over a major part of the interface except perhaps in the vicinity of the surface of the geological medium where delaminations may occur due to radial deformations of the anchor. In the case of anchoring elements with low length to diameter ratios and/or high relative stiffness, the interface delaminations and cracking could be induced particularly in the basal region. Such defects could be induced by impact loads or thermal effects at load levels which are well below the pull-out capacity of the anchor. Other forms of interface degradation can include failure of the interface as a result of inelastic behaviour and degradation particularly along the cylindrical interface (Selvadurai and Boulon [1]).

In this paper we examine the axisymmetric problem of the load transfer from a cylindrical anchor to a halfspace region particularly for the situation where a delamination has occured in the form of an open circular crack at the base of the cylindrical anchor (Figure 1). The analysis of the problem is approached via a boundary element formulation which takes into consideration the bi-material nature of the domain and the singular character of the stress field at the tip of the crack which extends to the geological medium. The results of the numerical analysis illustrate the influence of the extent of stable basal cracking on the elastic stiffness of the anchor and the crack opening and crack shearing mode stress intensity factors at the crack tip.

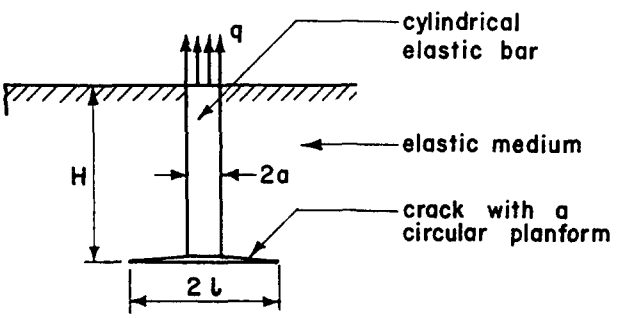

Figure 1. Cylindrical anchor with basal crack.

THE BOUNDARY ELEMENT METHOD

The boundary integral equation applicable to axisymmetric deformations of the elastic medium can be written in the form (see e.g., Brebbia et al. [2])

$$c_{\ell k} u_k^{(\alpha)} + \int_{\Gamma_{(\alpha)}} \left\{ P_{\ell k}^{*(\alpha)} u_k^{(\alpha)} - u_{\ell k}^{*(\alpha)} P_k \right\} \frac{r}{r_i} d\Gamma = 0 \quad (1)$$

where $P_{\ell k}^{*(\alpha)}$ and $u_{\ell k}^{*(\alpha)}$ are the traction and displacement fundamental solutions which are given in [2]. In (1) $c_{\ell k}$ is a constant ($c_{ij} = 0$, if the point is outside the body; $c_{ij} = \delta_{ij}$, if the point is inside the body and $c_{ij} = \delta_{ij}/2$, if the point is located at a smooth boundary). By discretizing the boundaries Γ_α into boundary elements, the boundary integral equation (1) can be replaced by its discretized equivalent. Upon completion of the integrations and summations, the discretized equation can be written in matrix form

$$\left[\mathbf{H}^{(\alpha)}\ \mathbf{H}_I^{(\alpha)}\right] \begin{bmatrix} \mathbf{u}^{(\alpha)} \\ \mathbf{u}_I^{(\alpha)} \end{bmatrix} = \left[\mathbf{M}^{(\alpha)}\ \mathbf{M}_I^{(\alpha)}\right] \begin{bmatrix} \mathbf{P}^{(\alpha)} \\ \mathbf{P}_I^{(\alpha)} \end{bmatrix} \quad (2)$$

where $\mathbf{u}_I^{(\alpha)}$ and $\mathbf{P}_I^{(\alpha)}$ are respectively the displacements and tractions at the interface between the cylindri-

[1]Department of Civil Engineering and Applied Mechanics, McGill University, Montreal, P.Q., Canada, H3A 2K6.

cal anchor and the geological medium. For complete bonding at the interface

$$\mathbf{u}_I^{(b)} = \mathbf{u}_I^{(m)} = \mathbf{u}_I \;\; ; \;\; \mathbf{P}_I^{(b)} = -\mathbf{P}_I^{(m)} = \mathbf{P}_I \qquad (3)$$

Using the above constraints, the boundary element matrix equation (2) can be written as

$$\begin{bmatrix} \mathbf{H}^{(b)} & \mathbf{H}_I^{(b)} & 0 \\ 0 & \mathbf{H}_I^{(m)} & \mathbf{H}^{(m)} \end{bmatrix} \begin{bmatrix} \mathbf{u}^{(b)} \\ \mathbf{I} \\ \mathbf{u}^{(m)} \end{bmatrix}$$

$$= \begin{bmatrix} \mathbf{M}^{(b)} & \mathbf{M}_I^{(b)} & 0 \\ 0 & -\mathbf{M}_I^{(m)} & \mathbf{M}^{(m)} \end{bmatrix} \begin{bmatrix} \mathbf{P}^{(b)} \\ \mathbf{P}_I \\ \mathbf{P}^{(m)} \end{bmatrix} \qquad (4)$$

which is the resulting bi-material boundary element matrix equation for the anchor-elastic medium system.

THE MODELLING OF THE BASAL FRACTURE

In the present study we consider the possible existence of a flat circular crack at the base of the anchor as shown in Figure 1. The presence of such cracks can lead to the initiation of brittle fracture at the boundary of the crack region. Boundary element techniques can be used to evaluate the "stress intensity factors" at the crack boundaries. The stress intensity factors reflect the states of stress associated with the method of loading of the crack tip. When considering the local geometry of the circular crack tip, the state of stress can be modelled by a state of two dimensional plane strain. Considering classical developments for linear elastostatic crack problems we observe that the stresses at the tip of a plane crack in a single material region exhibits a singularity of the $1/\sqrt{r}$ where r represents the radial distance from the crack tip. The displacements near a crack tip which is located along the y-axis (Figure 2) are given by

$$\frac{4Gu_y}{\sqrt{r/2\pi}} = K_1 \left\{ (5-8\nu)\cos\frac{\Theta}{2} - \cos\frac{3\Theta}{2} \right\} + K_{II} \left\{ (9-8\nu)\sin\frac{\Theta}{2} + \sin\frac{3\Theta}{2} \right\} \qquad (5)$$

$$\frac{4Gu_x}{\sqrt{r/2\pi}} = K_1 \left\{ (7-8\nu)\sin\frac{\Theta}{2} - \sin\frac{3\Theta}{2} \right\} - K_{11} \left\{ (3-8\nu)\cos\frac{\Theta}{2} + \cos\frac{3\Theta}{2} \right\} \qquad (6)$$

In (5) and (6) the parameters K_I and K_{II} represent the stress intensity factors for the crack opening and crack shearing modes of deformation. The results (5) and (6) also imply $\sqrt{r}$- and $1/\sqrt{r}$-type variation in the displacements and stresses, respectively, at the crack tip. In the finite element modelling of crack behaviour, the quarter-point element can be used to model the $\sqrt{r}$-type variation in the displacements i.e.,

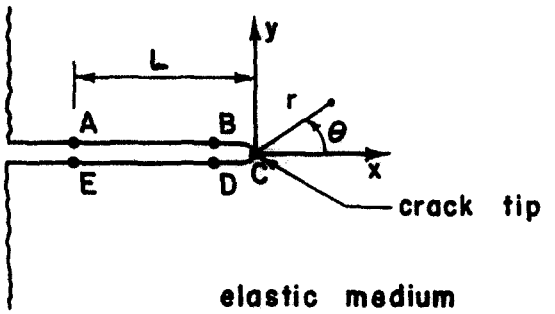

Figure 2. Crack tip geometry.

$$\left.\begin{matrix} u_i^{(\alpha)} \\ t_i^{(\alpha)} \end{matrix}\right\} = b_0 + b_1\sqrt{r} + b_2 r \qquad (7)$$

where b_0, b_1 and b_2 are constants. If the same type of element is implemented in the boundary element scheme to generate a quarter point boundary element, the tractions do not exhibit the appropriate singular behaviour at the crack tip. To alleviate this limitation, Cruse and Wilson [3] developed a singular traction quarter point boundary element where the variation of tractions are expressed in the form

$$t_i^{(\alpha)} = \frac{c_0}{\sqrt{r}} + c_1 + c_2\sqrt{r} \qquad (8)$$

where c_0, c_1 and c_2 are constants. The traction variation (8) is obtained by multiplying the traction variation given by (7) by $\sqrt{L/r}$ where L is the length of the crack tip element (Figure 2). The accuracy and performance of both types of crack tip elements has been investigated by a number of authors including Selvadurai and Au [4]. These studies indicate that the results derived via the singular traction quarter point element compare very accurately with known exact solutions.

To obtain the stress intensity factors K_I and K_{II} one could apply the displacement correlation method which utilizes the nodal displacements obtained from the crack tip elements at opposite sides of the crack. Referring to the Figure 2, the stress intensity factors can be derived from the following general relationships

$$K_I = \frac{G}{(1-\nu)}\sqrt{\frac{\pi}{2L}}\{[u_x(B) - u_x(D)] + u_x(E) - u_x(A)\} \qquad (9)$$

$$K_{II} = \frac{G}{(1-\nu)}\sqrt{\frac{\pi}{2L}}\{4[u_y(B) - u_y(D)] + u_y(E) - u_y(A)\} \qquad (10)$$

where L is the length of the crack-tip element and A, B, C, D and E are the nodes of the two crack tip elements on either side of the crack. The boundary

element scheme can be used to evaluate the relative magnitudes of the stress intensity factors K_I and K_{II} at the crack tip. In order to determine the conditions at which the crack will extend in a brittle fashion it is necessary to specify a fracture extension criteria. Such brittle fracture criteria will contain experimentally derived critical values of the stress intensity factors (K_I^c and K_{II}^c) which are utilized either individually or in a mixed mode. The fracture toughness of the brittle material under the separate modes of fracture propagation are directly related to K_I^c and K_{II}^c.

BOUNDARY ELEMENT MODELLING OF THE EMBEDDED BAR PROBLEM

Prior to the solution of the problem related to the axial loading of the embedded anchor with the base delamination, the accuracy of the boundary element scheme was verified by comparison with known exact solutions and numerical solutions. The accuracy in the evaluation of the mode I stress intensity factor at the crack tip was assessed by comparison with the exact closed form results for a penny-shaped crack located in an elastic solid of infinite extent (Sneddon [5]). It is found that the boundary element scheme can evaluate the stress intensity factor at the crack tip to within an accuracy of 0.5%. The discrepancy is within computational efficiency desired, and could be partly attributed to the finite nature of the domain used in the boundary element modelling.

We now apply the boundary element technique to examine the problem of the axial loading of an elastic anchor embedded in an elastic medium and weakened by a crack with a circular planform, located at the base of the anchor. The upper surface of the anchor is assumed to be at the surface of the halfspace region. The anchor is subjected to a uniform axial stress of magnitude q (i.e., $P = \pi q a^2$). The boundary element discretization adopted in the analysis is shown in Figure 3. The outer boundaries of the elastic medium are located at finite distances from the embedded elastic anchor sufficient to simulate the effects of a halfspace region to within the accuracies discussed previously. The boundary supports are constrained with zero shear tractions. Special crack tip elements are incorporated at the boundary of the crack. Since the cylindrical anchor is subjected to a uniform axial stress at the exterior boundary the axial displacements on any plane z=const., will in general be non-uniform. Consequently, the axial displacement within the anchor can be defined in an average sense according to the following

$$\Delta = \frac{1}{a}\int_0^a u_z(r,0)\,dr \qquad (11)$$

The introduction of the average displacement measure enables the calculation of the effective stiffness of the anchor in a realistic and specific manner, particularly for situations where $E_b \to E_m$. For convenience in the presentation of the numerical results, we shall consider numerical results for the case where the Poisson's ratios for the elastic anchor and the elastic medium are both equal.

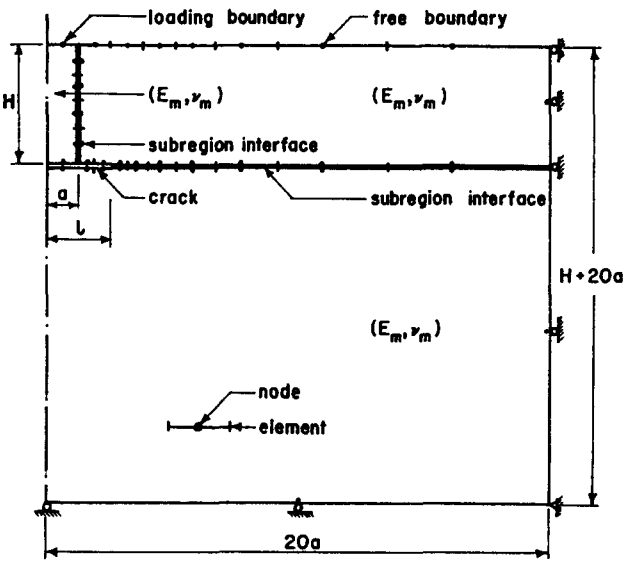

Figure 3. Boundary element discretization.

NUMERICAL RESULTS

The variables in the problem include the following: the anchor-elastic medium modulus ratio (E_b/E_m) the length to radius ratio of the cylindrical anchor (H/a), the radius of the crack region in relation to the radius of the cylindrical anchor (ℓ/a) and the Poisson's ratios of the elastic medium and the elastic anchor (ν_m, ν_b). For purposes of illustration, the numerical results are developed for the specific case in which $\nu_m = \nu_b = 0.25$. The numerical analysis can of course be extended to cover other specific combinations of the Poisson's ratios ν_m and ν_b.

The Table 1 gives values for the axial stiffness of a cylindrical anchor which is embedded in an elastic halfspace region in the absence of a basal fracture. The results derived from the boundary element scheme are compared with equivalent results obtained by Karasudhi et al. [6] and Selvadurai and Rajapakse [7], for the special case when $\nu_m = 0.25$; $\nu_b = 0.25$. The study by Karasudhi et al. [6] utilizes the fundamental solution given by Mindlin [8] to develop the discretized compatibility equations at the boundary of the anchor-elastic medium interface for the situation where the state of stress in the anchor is assumed to be uniaxial. Selvadurai and Rajapakse [7] used a variational procedure where the displacements of the anchor with a uniaxial state of stress are prescribed to within a set of arbitrary constants. The results for the non-dimensional axial displacement of the anchor derived via these two methods agree very closely and the maximum discrepancy does not exceed 5%. The numerical results for the non-dimensional axial displacement of the anchor derived via the boundary element scheme

are also shown in Table 1. The maximum discrepancy between the results derived via the boundary element scheme and the results given by Karasudhi et al. [6] or Selvadurai and Rajapakse [7] does not exceed 2.5%. This discrepancy can be attributed to the fact that in the boundary element scheme the region is specified to be of finite extent whereas in the other numerical schemes the elastic medium is modelled a a halfspace region. In the limit when $E_b \rightarrow E_m$, the dependence on H/a disappears and the problem reduces to that of the surface loading of a homogeneous elastic halfspace region by a circular loading of intensity q and radius a. The classical solution to Boussinesq's problem for the surface loading of a halfspace region by a concentrated load can be integrated to obtain the appropriate results for the surface displacements (see e.g., Timoshenko and Goodier, [9]). The analytical solutions for the surface displacements at the centre and edge of the loaded region are given by

$$[u_z(0,0)\,;\; u_z(a,0)] = \frac{2qa\,(1-\nu_m^2)}{E_m}\left[1;\; \frac{2}{\pi}\right]$$

For the special case when $\nu = 0.25$ we obtain

$$\frac{[u_z(0,0)]_{\text{analytical}}}{[u_z(0,0)]_{\text{BEM}}} = 0.9904 \quad ;$$

$$\frac{[u_z(a,0)]_{\text{analytical}}}{[u_z(a,0)]_{\text{BEM}}} = 0.9969$$

The above results indicate that the boundary element technique can be used to evaluate, reasonably accurately, the axial stiffness of the embedded anchor. The Figures 4 and 5 illustrate the manner in which the axial stiffness of the embedded anchor with a basal fracture is influenced by the anchor-elastic medium modular ratio (E_b/E_m), the relative dimensions of the basal crack (ℓ/a) and the geometry of the anchor (H/a). As is evident, the basal crack has the overall effect of reducing the axial stiffness of the anchor. As $E_b \rightarrow E_m$, the problem reduces to that of the surface loading of a homogeneous elastic halfspace with a crack, by a circular loading of intensity q and radius a. In this sense, the stiffness of the halfspace region is influenced by H/a, the depth of location of the crack and the geometry of the crack ℓ/a. Although the crack has a minor influence on the surface stiffness of the halfspace region it is evident that as H/a decreases the effective stiffness also decreases.

We shall now focus attention on the stress intensity factors which occur at the tip of the cracked region. The Figures 6 and 7 illustrate the variations in the stress intensity factors for the crack opening (K_I) and crack shearing (K_{II}) modes, as a function of the anchor-elastic medium modular ratio (E_b/E_m), the geometry of the anchor (H/a) and the relative dimensions of the crack region (ℓ/a). It is evident that the dominant mode for fracture initiation is the crack opening mode. In all instances pertaining to variable crack lengths (ℓ/a in the range 1 to 2) $K_I > K_{II}$. The value of K_I and K_{II} when $\ell/a \simeq 1$, has to be interpreted with some clarification. In the instance when the crack boundary terminates in a region with different elastic properties the stress singularity at the crack tip exhibits oscillatory phenomena (see e.g., Kassir and Sih [10]). This is in contrast to the regular behaviour (i.e., a stress singularity of order $1/\sqrt{r}$ where r is the distance from the crack tip) encountered at a crack tip located in a single medium. Consequently the stress intensity factors evaluated for $\ell/a = 1$ should be interpreted as a "smeared average" of the oscillatory phenomena at the crack tip. The boundary element method gives the regular estimates for K_I and K_{II} when $(\ell/a) > 1$. Following the investigations on bonded disc anchors conducted by Selvadurai [11] it may also be noted that the oscillatory singularities have virtually no influence on the axial stiffness of the embedded disc anchor. Finally, it may be observed that for all choices of ℓ/a, the stress intensity factors decrease as H/a increases. This can be attributed to the load transfer effect along the bonded length of the anchor.

Table 1: Comparison of non-dimensional axial displacement of an elastic anchor embedded in an elastic halfspace

(a) $H/a = 10 \quad \nu_b = \nu_m = 0.25$

E_b/E_m	$\Delta E_m/qa$		
	Ref.[6]	Ref.[7]	Present Study
1			1.6578
5	0.7896	0.7729	0.7912
10	0.6256	0.6043	0.6071
50	0.4019	0.3904	0.3893
100	0.3618	0.3431	0.3521
500	0.3266	0.3182	0.3195
1000	0.3220	0.3137	0.3152
10,000	0.3167	0.3096	0.3021

(b) $H/a = 5 \quad \nu_b = \nu_m = 0.25$

E_b/E_m	$\Delta E_m/qa$		
	Ref.[6]	Ref.[7]	Present Study
1			1.6578
5	0.8261	0.8140	0.8250
10	0.6893	0.6812	0.6715
50	0.5285	0.5457	0.5194
100	0.5049	0.5232	0.4972
500	0.4850	0.5043	0.4791
1000	0.4820	0.5019	0.4768
10,000	0.4810	0.4995	0.4667

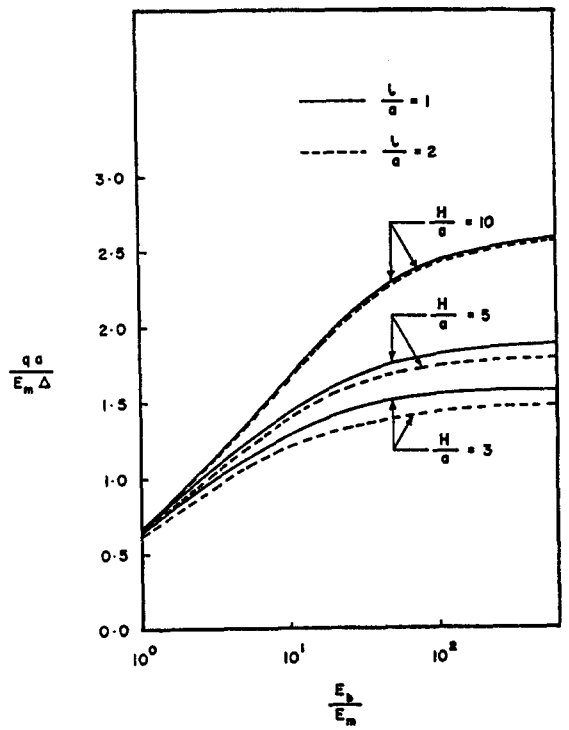

Figure 4. Axial stiffness of the anchor with a basal crack.

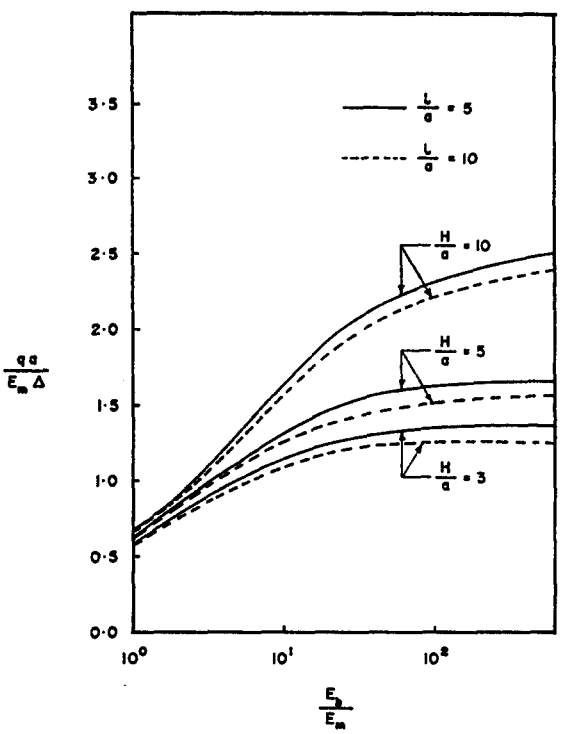

Figure 5. Axial stiffness of the anchor with a basal crack.

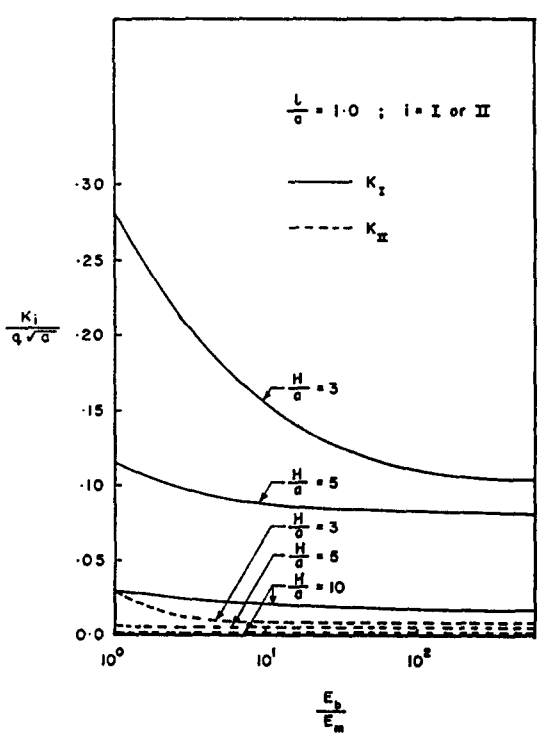

Figure 6. Stress intensity factors at the basal crack.

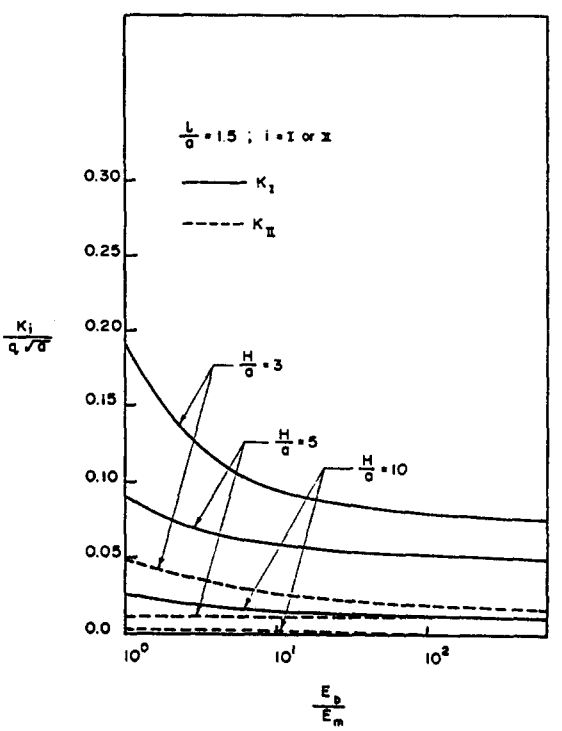

Figure 7. Stress intensity factors at the basal crack.

CONCLUSIONS

In the mechanical response of embedded anchors it is usually assumed that the interface between the anchor and the surrounding geological medium exhibits perfect bonding. This paper focusses on the situation where imperfect bonding can occur at the basal plane of the anchor leading to the development of a crack with a circular planform. It is shown that the boundary element technique can be successfully applied to evaluate the stiffness of the embedded anchor and the stress intensity factors at the tip of the basal crack. The stress intensity factor is an indicator of the propensity for crack propagation. At the basal crack the stress intensity factor in the crack opening mode is consistently greater than that for the crack shearing mode, for all choices of the anchor-elastic medium modulus ratio (E_b/E_m), anchor geometry ratio (H/a) and basal crack geometry (ℓ/a). It should be noted that if the crack were to extend, the orientation of the crack path will deviate from the simple circular planform stable basal crack configuration assumed in the modelling. The boundary element technique, however, can be readily adopted for the study of crack extension into the elastic rock mass region due to the attainment of critical criteria for the initiation and extension of fracture. The orientation of the crack extension can also be determined by specifying, an orientation of crack extension criterion. The boundary element technique can be conveniently adopted for iterative techniques associated with such analysis. The results provided in this study can also be used as guidelines for the assessment of the extent of stable basal cracks which can occur in rock anchoring devices which can be subjected to dynamic and other tensile loads.

APPENDIX

The fundamental solutions for the axisymmetric problem can be written as

$$u_{rr}^{*(\alpha)} = C_1 \left[\left\{ \frac{4(1-\nu_\alpha)(\rho^2+z^{-2})-\rho^2}{2r\overline{R}} \right\} K(m) - \left\{ \frac{(7-8\nu_\alpha)}{4r}\overline{R} - \frac{e^4-z^{-4}}{4r\overline{R}^3 m_1} \right\} E(m) \right] \quad (A1)$$

$$u_{rz}^{*(\alpha)} = C_1 \overline{z} \left[\frac{(e^2+z^{-2})}{2\overline{R}^3 m_1} E(m) - \frac{1}{2\overline{R}} K(m) \right] \quad (A2)$$

$$u_{zr}^{*(\alpha)} = C_1 r_i \overline{z} \left[\frac{(e^2-z^{-2})}{2r\overline{R}^3 m_1} E(m) + \frac{1}{2r\overline{R}} K(m) \right] \quad (A3)$$

$$u_{zz}^{*(\alpha)} = C_1 r_i \left[\frac{(3-4\nu_\alpha)}{\overline{R}} K(m) + \frac{z^{-2}}{\overline{R}^3 m_1} E(m) \right] \quad (A4)$$

where

$$\overline{z} = z - z_i;\ \overline{r} = r + r_i;\ \rho^2 = r^2 + r_i^2$$

$$e^2 = r^2 - r_i^2;\ \overline{R}^2 + \overline{z}^2;\ C_1 = 1/4\pi G_\alpha (1-\nu_\alpha)$$

and $K(m)$ and $E(m)$ are, respectively, the complete elliptic integrals of the first and second kinds where $m = 4rr_i/\overline{R}^2$ and $m_1 = 1 - m$. The corresponding components of the fundamental solution for the traction $P_{ik}^{*(\alpha)}$ can be obtained by the proper manipulation of the results (A1) to (A4).

REFERENCES

1. Selvadurai, A.P.S. and Boulon, M.J., Boundary element modelling of the mechanics of a near surface cylindrical rigid anchor, *Numerical Models in Geomechanics*, (G.N. Pande and S. Pietruszczak, Eds.) *Proc. 4th Int. Symp. on Numerical Models in Geomech.*, NUMOG IV, Swansea, **2**, pp.629-643 (1992).
2. Brebbia, C.A., Telles, J.C.F. and Wrobel, L.C., *Boundary Element Techniques*, Springer Verlag, Berlin (1984).
3. Cruse, T.A. and Wilson, R.B., Boundary integral equation methods for elastic fracture mechanics, *AFSOR-TR-0355, 10-11* (1977).
4. Selvadurai, A.P.S. and Au, M.C., Numerical modelling of bridged flaws in fibre reinforced plates, *Proc. of Int. Conf. Computer Aided Assessment of Localized Damage*, pp.211-230 (1990).
5. Sneddon, I.N., The stress distribution in the neighbourhood of a crack in an elastic solid, *Proc. Roy. Soc. Ser. A*, **187**, pp.229-260 (1946).
6. Karasudhi, P., Rajapakse, R.K.N.D. and Liyanage, K.K., A reconsideration of load transfer problems involving a halfspace, *Trans. Can. Soc. Mech. Eng.*, **8**, 219-226 (1984).
7. Selvadurai, A.P.S. and Rajapakse, R.K.N.D., Axial stiffness of anchoring rods embedded in elastic media, *Canadian Jnl. Civil Engineering*, Vol.17, pp.321-328 (1990).
8. Mindlin, R.D., Force at a point in the interior of a semi-infinite solid, *Physics*, **7**, pp.195-202 (1936).
9. Timoshenko, S.P. and Goodier, J.N., *Theory of Elasticity*, McGraw Hill, New York (1970).
10. Kassir, M.K. and Sih, G.C., *Three-Dimensional Crack Problems, Mechanics of Fracture Vol.2*, Noordhoff International Publ., Leyden, The Netherlands (1975).
11. Selvadurai, A.P.S., The influence of a boundary fracture on the elastic stiffness of a deeply embedded anchor plate, *Int. J. Numerical and Analytical Methods in Geomech.*, **13**, pp.159-170 (1989).